
¹⁴C-Methionine Uptake as a Potential Marker of Inflammatory Processes After Myocardial Ischemia and Reperfusion

Junichi Taki¹, Hiroshi Wakabayashi¹, Anri Inaki¹, Kyoko Imanaka-Yoshida², Michiaki Hiroe³, Kazuma Ogawa⁴, Miyako Morooka⁵, Kazuo Kubota⁵, Kazuhiro Shiba⁶, Toshimichi Yoshida², and Seigo Kinuya¹

¹Department of Nuclear Medicine, Kanazawa University Hospital, Kanazawa, Japan; ²Department of Pathology and Matrix Biology, Mie University School of Medicine, Tsu, Japan; ³Department of Cardiology, National Center for Global Health and Medicine, Tokyo, Japan; ⁴Graduate School of Natural Science and Technology, Kanazawa University, Kanazawa, Japan; ⁵Division of Nuclear Medicine, Department of Radiology, National Center for Global Health and Medicine, Tokyo, Japan; and ⁶Division of Tracer Kinetics, Advanced Science Research Center, Kanazawa University, Kanazawa, Japan

A relationship between L-[methyl-¹¹C]methionine (¹¹C-methionine) uptake and angiogenesis has been suggested in gliomas. However, methionine uptake in myocardial ischemia and reperfusion has received little attention. We investigated the serial changes and mechanisms of ¹⁴C-methionine uptake in a rat model of myocardial ischemia and reperfusion. **Methods:** The left coronary artery was occluded for 30 min, followed by reperfusion for 1–28 d. At the time of the study, ¹⁴C-methionine (0.74 MBq) and ²⁰¹Tl (14.8 MBq) were injected intravenously at 20 and 10 min before sacrifice, respectively. One minute before sacrifice, the left coronary artery was reoccluded, and ^{99m}Tc-hexakis-2-methoxyisobutylisonitrile (150–180 MBq) was injected to verify the area at risk. Histologic sections of the heart were immunohistochemically analyzed using anti-CD68, anti-smooth-muscle α -actin (SMA), and antitroponin I and compared with the autoradiography findings. **Results:** Both ¹⁴C-methionine (uptake ratio, 0.71 ± 0.13) and ²⁰¹Tl uptake were reduced in the area at risk at 1 d after reperfusion. However, 3 d after reperfusion, an increased ¹⁴C-methionine uptake (1.79 ± 0.23) was observed corresponding to the area of still-reduced ²⁰¹Tl uptake, and the ¹⁴C-methionine uptake gradually declined until 28 d. The increased ¹⁴C-methionine uptake area at 3 and 7 d corresponded well to the macrophage infiltrations demonstrated by positive CD68 staining. Anti-SMA staining appeared at 7 d, after which CD68 staining was gradually replaced by the SMA staining, suggesting that methionine uptake in the early phase after ischemia and reperfusion might reflect inflammatory activity. **Conclusion:** ¹⁴C-methionine accumulated in the infarcted area, and its uptake corresponded closely to macrophage infiltration at 3–7 d after reperfusion. Methionine imaging may be useful for inflammatory imaging early after myocardial infarction.

Key Words: methionine; myocardial ischemia; reperfusion; myocardial infarction; macrophage

J Nucl Med 2013; 54:431–436

DOI: 10.2967/jnumed.112.112060

L-[methyl-¹¹C]methionine (¹¹C-methionine) has been used for the evaluation of various tumors, especially for brain tumors because of its low physiologic uptake by brain tissue (1). The uptake mechanism of ¹¹C-methionine in tumors depends mainly on carrier-mediated transport systems (2) and correlates with the proliferative activity (3) and microvessel density (4), which reflects angiogenesis. However, because it has also been reported that in human glioma the cell density contributes more to ¹¹C-methionine uptake than does the microvessel density (5,6), the mechanism of ¹¹C-methionine uptake remains to be clarified.

Other than in tumors, radiolabeled amino acids including ¹¹C-methionine have been investigated in only a few studies. In canine myocardium, ¹³N- and ¹¹C-labeled L-amino acid kinetics were investigated in the evaluation of the amino acid metabolism (7,8). In pacing-induced ischemia, ¹³N-glutamine and ¹³N-alanine that accumulated in the ischemic area were shown to be perfusion defects by ¹³N-ammonia (7). During low-flow ischemia and after reperfusion, retention of ¹³N-labeled amino acids was higher than in controls (8).

Recently, we reported that ¹¹C-methionine uptake is elevated in the infarcted areas in patients with acute myocardial infarction and successful percutaneous coronary intervention (9). We speculated that this elevated uptake may reflect the early phase of damage healing, which involves, for instance, inflammatory processes and angiogenesis.

Therefore, to evaluate the underlying mechanisms of methionine uptake in myocardial infarction, we explored its spatial and temporal changes after myocardial ischemia and

Received Aug. 1, 2012; revision accepted Sep. 19, 2012.

For correspondence or reprints contact: Junichi Taki, Department of Nuclear Medicine, Kanazawa University Hospital, 13-1 Takara-Machi, Kanazawa, 920-8641, Japan.

E-mail: taki@med.kanazawa-u.ac.jp

Published online Jan. 15, 2013.

COPYRIGHT © 2013 by the Society of Nuclear Medicine and Molecular Imaging, Inc.

reperfusion using ^{14}C -methionine in a rat model of acute ischemia and reperfusion. Furthermore, we correlated the spatiotemporal uptake pattern of methionine to the histopathologic features during the healing process of acute myocardial infarction.

MATERIALS AND METHODS

Animal Model of Acute Ischemia and Reperfusion

All experimental procedures involving animals were conducted in accordance with the institutional guidelines set by the Institute for Experimental Animals, Kanazawa University Advanced Science Research Center. Eight- to 10-wk-old male Wistar rats ($n = 28$) were anesthetized with an intraperitoneal administration of 40 mg of pentobarbital per kilogram and ventilated mechanically with room air. After left thoracotomy and exposure of the heart, a 7-0 polypropylene suture on a small curved needle was passed through the myocardium beneath the proximal portion of the left coronary artery (LCA), and both ends of the suture were passed through a small vinyl tube to make a snare. The suture material was pulled tight against the vinyl tube to occlude the LCA. Myocardial ischemia was confirmed by regional cyanosis of the myocardial surface and ST-segment elevation on the electrocardiogram. After a 30-min interval of LCA occlusion, reperfusion was obtained by release of the snare and confirmed by a myocardial blush over the area at risk. The snare was left loose on the surface of the heart until just before sacrifice, when it was retightened to identify the area at risk (10). Groups of animals were studied at 1 ($n = 6$), 3 ($n = 5$), 7 ($n = 5$), 14 ($n = 6$), and 28 d ($n = 6$) after reperfusion. At the time of the study, ^{14}C -methionine (0.74 MBq) (methionine, L-[methyl- ^{14}C] [American Radiolabeled Chemicals, Inc.]; specific activity, 2.04 GBq/mmol; radiochemical purity, >98%) was administered via the tail vein at 20 min before sacrifice. Then ^{201}Tl (14.8 MBq) was administered at 10 min before sacrifice to measure the infarcted area. One minute before sacrifice, 150–180 MBq of $^{99\text{m}}\text{Tc}$ -hexakis-2-methoxyisobutylisonitrile (MIBI) was injected via the tail vein just after the reocclusion of the proximal portion of the LCA for delineation of the area at risk. One minute later, the rat was euthanized and the heart was removed for analysis (Fig. 1). The excised heart was rinsed in saline, frozen in isopentane, cooled in dry ice, and embedded in methyl cellulose. Serial short-axis heart sections of 20- μm thickness were obtained by sectioning on a cryostat to create a series of rings for autoradiography.

Triple-Tracer Autoradiography

Triple-tracer autoradiography of the left ventricular short-axis slices was performed for the assessment of ^{14}C -methionine uptake, ^{201}Tl uptake, and the ischemic area ($^{99\text{m}}\text{Tc}$ -MIBI image). The first autoradiographic exposure on an imaging plate (BAS-MS; Fuji Film) was performed for 15–20 min to visualize the area at risk expressed by $^{99\text{m}}\text{Tc}$ -MIBI distribution at 1–2 h after sacri-

fice. Three days later (12 half-lives of $^{99\text{m}}\text{Tc}$), the second exposure was made for 5–8 h to image the distribution of ^{201}Tl . One month later, the third exposure, for visualization of methionine uptake, was performed for 1–2 wk.

Data Analysis

Tracer accumulations were evaluated in 3 myocardial slices spaced 1 mm apart from one another at the mid ventricular level. The distribution of the tracers was determined by analysis of the digitized autoradiography. The photostimulated luminescence in each pixel (50 \times 50 μm) was determined using a bioimaging analyzer (BAS-5000; Fuji Film). For quantitative analysis, the uptake values of each region of interest (ROI) were expressed as the background-corrected photostimulated luminescence per unit area (0.25 mm^2). A background ROI was set adjacent to the left ventricle. Ischemic and normally perfused areas were defined from the $^{99\text{m}}\text{Tc}$ -MIBI image, and these ROIs were applied to both the ^{14}C -methionine and the ^{201}Tl images to evaluate the uptake of ^{14}C -methionine and ^{201}Tl . The ischemic area was divided into salvaged and infarcted areas arbitrarily by ^{201}Tl uptake ($\geq 60\%$ uptake and $< 60\%$ of normally perfused area, respectively) (11). A significant ^{14}C -methionine uptake area was also defined manually as an ROI. The ^{14}C -methionine uptake ratio in an ischemic area was calculated by dividing the uptake value in an ischemic area by that of a normally perfused area. ^{14}C -methionine uptake ratios of salvaged and infarcted areas were also calculated. The ratio of ^{14}C -methionine uptake ROI area to ischemic ROI area was defined as the percentage of the ^{14}C -methionine uptake area. All parameters in each rat were expressed as the average value obtained from the analysis of 3 representative slices.

Immunohistochemical Staining

Short-axis frozen sections (5 μm thick) adjacent to the slices for autoradiography were mounted on slides. They were washed with phosphate-buffered saline and immunostained with mouse antirat CD68 macrophage antibody (clone ED1; MBA Biomedical) to determine macrophage infiltration after ischemia and reperfusion. Viable cardiomyocytes were immunostained with rabbit polyclonal anticardiac troponin I antibody (Abcam). The following secondary antibodies were used: peroxidase-conjugated goat antirabbit IgG or antimouse IgG (MBL). A diaminobenzidine- H_2O_2 solution was used to demonstrate peroxidase-conjugated secondary antibody binding. Also, the slices were immunofluorescently double-stained with anticardiac troponin I antibody and either anti-CD68 or fluorescein isothiocyanate-conjugated anti-smooth-muscle α -actin (SMA) (clone 1A4; Sigma). The following secondary antibodies were also used: fluorescein isothiocyanate-conjugated goat antimouse IgG (MBL) and Alexa Fluor 546 F (ab')₂ fragment of goat antirabbit IgG (H+L) (Molecular Probes). The samples were observed under a conventional fluorescent or light microscope (Olympus), and images were recorded with a cooled charge-coupled device camera. The immunofluorescent signals for each stain were converted into pseudocolor and superimposed using Photoshop (Adobe).

Statistical Analysis

All results were expressed as the mean \pm SD. Statistical analyses were performed using a Macintosh computer (Apple) with JMP software (8.0.1J). Group comparisons were performed using the Tukey-Kramer method to identify differences among groups. Comparisons of methionine uptake ratio between salvaged and infarcted areas at each reperfusion time were performed by paired

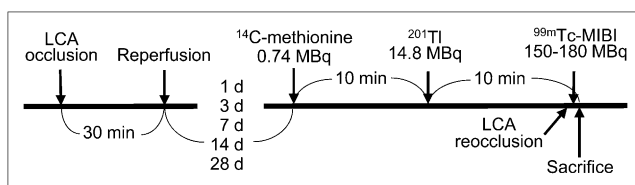


FIGURE 1. Experimental protocol.

t testing. A value of *P* less than 0.05 was considered statistically significant.

RESULTS

Size of Area with ¹⁴C-Methionine Uptake Against Area at Risk

The percentages of ¹⁴C-methionine uptake areas against area at risk in rats with 30-min ischemia and reperfusion at 3, 7, 14, and 28 d were similar ($41.1\% \pm 18.7\%$, $38.7\% \pm 11.4\%$, $52.9\% \pm 10.5\%$, and $44.0\% \pm 8.8\%$, respectively; *P* = not significant) (Fig. 2).

¹⁴C-Methionine and ²⁰¹Tl Uptake in Autoradiography

In the visual analysis, 1 d after reperfusion, the uptake of both ²⁰¹Tl and ¹⁴C-methionine was reduced in the area at risk. Thereafter, ²⁰¹Tl uptake recovered slightly but was still reduced, compared with the remote area from ischemia and reperfusion until 28 d after reperfusion (Fig. 3). In contrast, significantly increased ¹⁴C-methionine uptake was observed at 3 d after reperfusion in the area at risk, after which the uptake gradually decreased until 28 d after reperfusion. The distribution of ¹⁴C-methionine uptake roughly corresponded to the area with the more reduced ²⁰¹Tl uptake in the area at risk (Fig. 3).

In the quantitative analysis, the ²⁰¹Tl uptake ratio was severely suppressed at 1 d after reperfusion (0.35 ± 0.13) and was significantly increased at 3 d to 0.66 ± 0.10 . Thereafter, the ratios were similar at around 0.6–0.7: the uptake ratios at 7, 14, and 28 d were 0.70 ± 0.21 , 0.72 ± 0.09 , and 0.64 ± 0.09 , respectively. The ¹⁴C-methionine uptake ratio at 1 d after reperfusion was also suppressed (0.71 ± 0.13); however, uptake at 3 d after reperfusion increased significantly to 1.79 ± 0.23 . Subsequently, the ratios declined gradually until 28 d: the uptake ratios at 7, 14, and 28 d were 1.52 ± 0.20 , 1.31 ± 0.12 , and 1.12 ± 0.08 , respectively (Fig. 4). When ¹⁴C-methionine uptake was compared between salvaged and infarcted areas, the

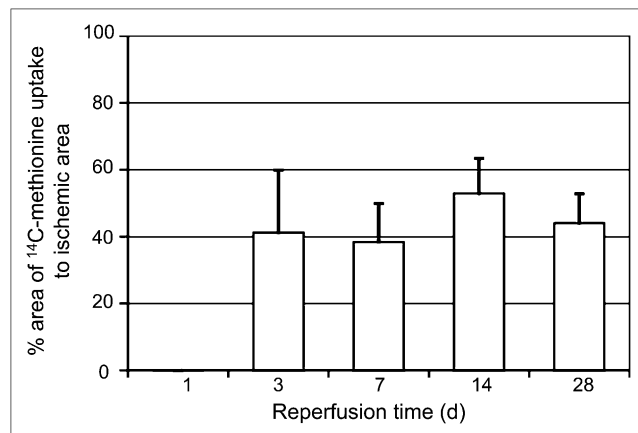


FIGURE 2. Time course of ¹⁴C-methionine uptake area against area at risk (% area). One day after reperfusion, no increased uptake of ¹⁴C-methionine was observed. Percentage area of methionine uptake was similar at 3, 7, 14, and 28 d after reperfusion.

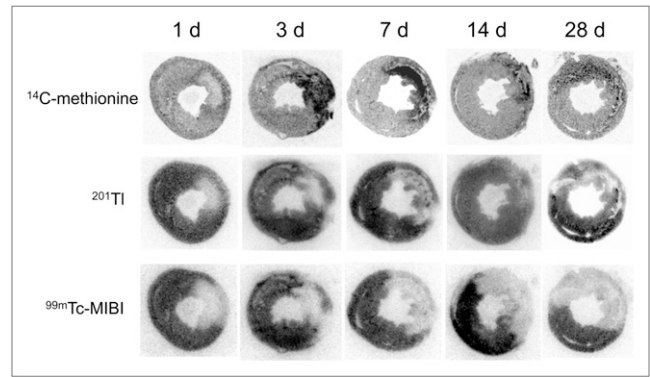


FIGURE 3. Autoradiography of ¹⁴C-methionine, ²⁰¹Tl, and ^{99m}Tc-MIBI. One day after reperfusion, both ¹⁴C-methionine and ²⁰¹Tl uptake decreased in area at risk (^{99m}Tc-MIBI defect). However, 3 d after reperfusion, ¹⁴C-methionine uptake increased significantly, followed by gradual reduction of uptake until 28 d. Distribution of ¹⁴C-methionine uptake roughly corresponds to reduced ²⁰¹Tl uptake area.

uptake ratios in the infarcted area were always higher than those in the salvaged area except for day 28: the ¹⁴C-methionine uptake ratios in infarcted and salvaged areas were, respectively, 0.88 ± 0.15 and 0.58 ± 0.094 at day 1 (*P* < 0.001), 1.87 ± 0.27 and 1.65 ± 0.25 at day 3 (*P* < 0.05), 1.60 ± 0.45 and 1.28 ± 0.26 at day 7 (*P* < 0.05), 1.38 ± 0.16 and 1.26 ± 0.10 at day 14 (*P* < 0.05), and 1.14 ± 0.097 and 1.10 ± 0.075 at day 28 (*P* = not significant).

Comparison of Autoradiography and Histopathologic Findings

The significant accumulation of ¹⁴C-methionine uptake in autoradiography corresponded closely to the area with positive immunohistopathologic staining with anti-CD68

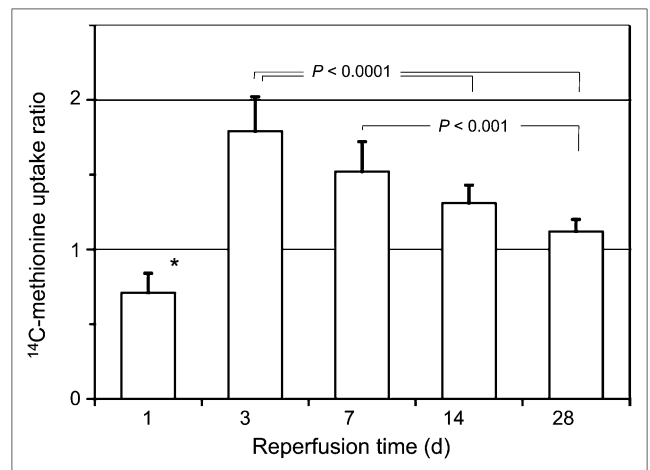


FIGURE 4. Time course of ¹⁴C-methionine uptake ratio. ¹⁴C-methionine uptake ratios were calculated by dividing ¹⁴C-methionine count density in area at risk by that of nonischemic area. ¹⁴C-methionine uptake reduced at 1 d after reperfusion but increased dramatically at 3 d, followed by gradual decrease to basal level until 28 d. **P* < 0.005 vs. 28 d, *P* < 0.0001 vs. 3, 7, and 14 d.

macrophage antibody at days 3 and 7 (Fig. 5). At 14 d, although anti-CD68 staining was greatly reduced, ^{14}C -methionine uptake continued to be detected in the reduced ^{201}Tl uptake area (Fig. 5).

Double immunofluorescent staining demonstrated that many CD68-positive macrophages accumulated in the absent part of troponin I-positive viable cardiomyocytes, peaked at day 3, and then gradually decreased after day 7 (Fig. 6).

No SMA-positive cells were found in the troponin I-negative area at day 3, whereas numerous SMA-positive cells were seen at day 7 (Fig. 6). The direct comparison of staining with anti-CD68 and anti-SMA (Fig. 7) showed that no SMA-positive cells were detected in the macrophage-rich area at 3 d, whereas numerous SMA-positive cells were present in the area where macrophages infiltrated at 7 d. At 14 d and later, with decreased numbers of macrophages, SMA-positive cells became predominant. Some of the SMA staining showed ringlike and tubular configurations, suggesting that SMA-positive cells may form luminal structures, possibly being recruited as the mural cells of newly formed blood vessels (Fig. 7).

DISCUSSION

The present study documented spatiotemporal profiling of ^{14}C -methionine uptake after myocardial ischemia and reperfusion in the myocardium with 30 min of ischemia and reperfusion in rats. ^{14}C -methionine accumulated in the infarcted area, and the uptake corresponded well to the macrophage infiltration at 3–7 d after reperfusion. Ac-

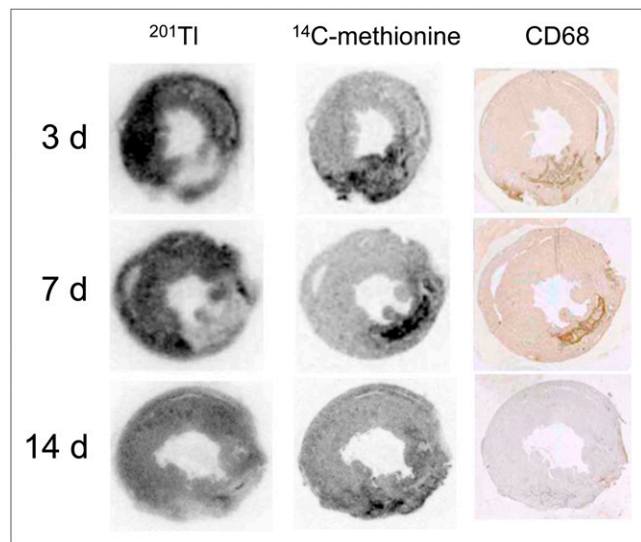


FIGURE 5. Comparison of ^{201}Tl and ^{14}C -methionine autoradiograms and anti-CD68 antibody staining (marker of macrophages). ^{14}C -methionine uptake was observed predominantly in area with reduced ^{201}Tl uptake at 3–14 d after reperfusion. On the other hand ^{14}C -methionine uptake corresponded closely to areas positive for anti-CD68 antibody at 3 and 7 d, whereas anti-CD68 antibody staining was weak when compared with ^{14}C -methionine uptake at 14 d.

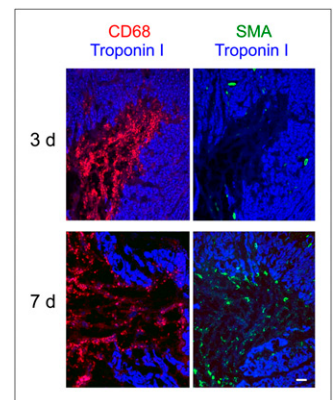


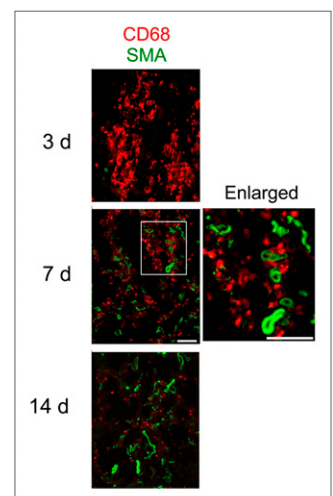
FIGURE 6. Double staining with cardiac troponin I and either anti-CD68 or anti-SMA of serial sections of heart at 3 and 7 d. Strong CD68 staining (red) was seen in troponin I (blue) defect area at 3 d. Anti-SMA-positive cells (green) were not observed at 3 d in troponin I defect area, but numerous SMA-positive cells were found at 7 d.

cordingly, methionine imaging may be useful for inflammatory imaging early after myocardial infarction.

In general, the process of myocardial tissue repair and healing after acute myocardial infarction is considered to consist of 4 phases based on the pathologic findings: cardiomyocyte death, acute inflammation, formation of granulation tissue, and scar formation (12). In the phase of acute inflammation, macrophages play multiple roles, including phagocytosis of the dead myocardial cells and debris and secretion of a variety of cytokines and growth factors (13). Then, monocyte-derived macrophages secrete a variety of fibrogenic and angiogenic growth factors and cytokines (14), inducing formation of granulation tissue and fibroblast proliferation, and fibroblasts undergo phenotypic changes expressing SMA, which are then called myofibroblasts. Myofibroblasts may be capable of assuming a variety of different roles, such as production of extracellular matrix proteins and late scar formation, wound contractile activity (15), and passive involvement in neovessel formation as mural cells such as pericytes expressing SMA (16).

Our previous study found significant ^{11}C -methionine uptake in the infarcted area, with reduced uptake of both ^{201}Tl

FIGURE 7. Double staining of anti-CD68 antibody (red) and anti-SMA (green) in area corresponding to ^{14}C -methionine uptake. At 3 d after reperfusion, strong staining of anti-CD68 antibody, but little anti-SMA staining was observed. At 7 d, significant amount of anti-SMA staining appeared in area of CD68 antibody red staining. Enlarged image of boxed area clearly demonstrated that some green staining showed ringlike or tubular configurations, suggesting formation of new blood vessels. At 14 d, anti-CD68 antibody stain decreased, whereas anti-SMA staining increased and still showed ringlike and tubular configurations. Scale bars = 100 μm .



and ^{18}F -FDG after oral glucose loading within 2 wk in patients with myocardial infarction and revascularization (9). However, the uptake of ^{14}C -methionine in the infarcted area was relatively low, possibly because of delayed reperfusion time after infarction and the procedure of ^{11}C -methionine PET. Our previous clinical data on the spatiotemporal uptake of ^{11}C -methionine in the infarcted areas may not have been clear from the aspect of histopathologic changes after ischemia and reperfusion.

In this study, we confirmed that the marked accumulation of ^{14}C -methionine in the infarcted areas corresponded to infiltration of numerous macrophages at 3 and 7 d after reperfusion. Although the number of CD68-positive cells decreased around day 7 and later, anti-SMA-positive cells appeared, suggesting that activated myofibroblasts may infiltrate the damaged sites in the process of tissue repair after 7–14 d of reperfusion. In addition, some of the anti-SMA staining showed ringlike or tubular configurations, suggesting that SMA-positive mural cells were recruited to newly formed vascular wall. Therefore, strong ^{14}C -methionine uptake within 1 wk of reperfusion would imply macrophage infiltration. Less marked uptake at the later stage might reflect, in part, activity by myofibroblasts and neovessel formation by mural cells as pericytes in granulomatous tissues, in addition to residual macrophage infiltration.

^{11}C -methionine imaging may become a valuable method to evaluate inflammatory processes about to undergo healing processes. The application of target radionuclide imaging of regional methionine uptake as proposed in the present study holds the potential to quantify the extent, amount, and localization of macrophage infiltrations early after myocardial infarction. Furthermore, the proposed imaging approach provides the opportunity to monitor novel therapeutic interventions directed toward mitigation of the severity of the inflammatory process and promotion of a proper transition to the reparative process and remodeling after myocardial infarction.

Acute inflammation can also be detected by ^{18}F -FDG PET, although, ^{18}F -FDG uptake due to inflammatory changes in myocardium might be obscured by physiologic ^{18}F -FDG uptake. Therefore, prolonged fasting, heparin loading, and dietary modification would be necessary to suppress the physiologic ^{18}F -FDG uptake in normal myocardium, as has been recommended in the evaluation of cardiac sarcoidosis (17). In this respect, ^{11}C -methionine PET has an advantage over ^{18}F -FDG PET because ^{11}C -methionine PET can be performed easily without any special preparation.

Although the current study demonstrated the changes in the spatiotemporal ^{14}C -methionine accumulation after myocardial ischemia and reperfusion, further study is needed to investigate the relationship between the early degree of ^{14}C -methionine uptake or temporal prolongation of the uptake and the later ventricular dilatation or remodeling and pump failure after myocardial infarction. Assessments as to whether interventional therapy aimed at

protecting against myocardial damage and ventricular remodeling is related to changes in ^{14}C -methionine uptake, and whether these really reflect the therapeutic effect, are also required.

This study had some limitations. First, direct evidence that ^{14}C -methionine accumulates in each macrophage was absent, because no histologic autoradiography was undertaken to evaluate which cells in the infarcted tissue accumulated ^{14}C -methionine. However, our pathologic and immunohistologic studies found inflammation cells to be mainly macrophages during acute inflammation at 3–7 d after reperfusion, whereas the areas of ^{14}C -methionine uptake corresponded to the infarcted tissue occupied by macrophages. Second, angiogenesis was not histopathologically confirmed, but we surmised that SMA-positive cells were myofibroblasts and mural cells were pericytes because some of the SMA staining showed ringlike and tubular configurations, suggesting luminal structures. Further study on ^{14}C -methionine accumulation in the SMA-positive cells is needed.

CONCLUSION

The present study clarified the spatiotemporal uptake pattern of ^{14}C -methionine after 30 min of ischemia and reperfusion. The current data demonstrated that, corresponding to the area with reduced ^{201}Tl uptake, strong ^{14}C -methionine uptake was observed after 3–7 d of reperfusion and declined gradually until 28 d after reperfusion. The immunohistologic examinations suggested that the methionine uptake might indicate macrophage infiltrations in infarcted areas. These findings would help to clarify the ^{11}C -methionine uptake in patients with acute myocardial infarction with reperfusion. In addition, methionine imaging may be useful for inflammatory imaging early after myocardial infarction.

DISCLOSURE

The costs of publication of this article were defrayed in part by the payment of page charges. Therefore, and solely to indicate this fact, this article is hereby marked “advertisement” in accordance with 18 USC section 1734. This work has been supported by grants in aid for scientific research (C-23591756 and 21590927) from the Ministry of Education, Culture, Sports, Science, and Technology, Japan; by a research grant for intractable diseases from the Ministry of Health, Labor and Welfare of Japan; by a grant from the Japan Foundation for the Promotion of the International Medical Center of Japan; and by a grant from the National Center for Global Health and Medicine (no. 21-126). No other potential conflict of interest relevant to this article was reported.

ACKNOWLEDGMENTS

We thank Miyuki Namikata for providing technical assistance.

REFERENCES

1. Cook GJ, Maisey MN, Fogelman I. Normal variants, artefacts and interpretative pitfalls in PET imaging with 18-fluoro-2-deoxyglucose and carbon-11 methionine. *Eur J Nucl Med*. 1999;26:1363–1378.
2. Crippa F, Alessi A, Serafini GL. PET with radiolabeled amino acid. *Q J Nucl Med Mol Imaging*. 2012;56:151–162.
3. Kato T, Shinoda J, Oka N, et al. Analysis of ¹¹C-methionine uptake in low-grade gliomas and correlation with proliferative activity. *AJNR*. 2008;29:1867–1871.
4. Kracht LW, Friese M, Herholz K, et al. Methyl-[¹¹C]-l-methionine uptake as measured by positron emission tomography correlates to microvessel density in patients with glioma. *Eur J Nucl Med Mol Imaging*. 2003;30:868–873.
5. Okita Y, Kinoshita M, Goto T, et al. ¹¹C-methionine uptake correlates with tumor cell density rather than with microvessel density in glioma: a stereotactic image-histology comparison. *Neuroimage*. 2010;49:2977–2982.
6. Arita H, Kinoshita M, Kagawa N, et al. ¹¹C-methionine uptake and intraoperative 5-aminolevulinic acid-induced fluorescence as separate index markers of cell density in glioma: a stereotactic image-histological analysis. *Cancer*. 2012;118:1619–1627.
7. Henze E, Schelbert HR, Barrio JR, et al. Evaluation of myocardial metabolism, with N-13- and C-11-labeled amino acids and positron computed tomography. *J Nucl Med*. 1982;23:671–681.
8. Barrio JR, Baumgartner FJ, Henze E, et al. Synthesis and myocardial kinetics of N-13 and C-11 labeled branched-chain L-amino acids. *J Nucl Med*. 1983;24:937–944.
9. Morooka M, Kubota K, Kadowaki H, et al. ¹¹C-methionine PET of acute myocardial infarction. *J Nucl Med*. 2009;50:1283–1287.
10. Taki J, Higuchi T, Kawashima A, et al. Effect of postconditioning on myocardial ^{99m}Tc-annexin-V uptake: comparison with ischemic preconditioning and caspase inhibitor treatment. *J Nucl Med*. 2007;48:1301–1307.
11. Sahul ZH, Mukherjee R, Song J, et al. Targeted imaging of the spatial and temporal variation of matrix metalloproteinase activity in a porcine model of postinfarct remodeling: relationship to myocardial dysfunction. *Circ Cardiovasc Imaging*. 2011;4:381–391.
12. Blankesteijn WM, Creemers E, Lutgens E, Cleutjens JP, Daemen MJ, Smits JF. Dynamics of cardiac wound healing following myocardial infarction: observations in genetically altered mice. *Acta Physiol Scand*. 2001;173:75–82.
13. Lambert JM, Lopez EF, Lindsey ML. Macrophage roles following myocardial infarction. *Int J Cardiol*. 2008;130:147–158.
14. Weihrauch D, Arras M, Zimmermann R, Schaper J. Importance of monocytes/macrophages and fibroblasts for healing of micronecroses in porcine myocardium. *Mol Cell Biochem*. 1995;147:13–19.
15. Serini G, Gabbiani G. Mechanisms of myofibroblast activity and phenotypic modulation. *Exp Cell Res*. 1999;250:273–283.
16. Armulik A, Genove G, Betsholtz C. Pericytes: developmental, physiological, and pathological perspectives, problems, and promises. *Dev Cell*. 2011;21:193–215.
17. Ohira H, Tsujino I, Yoshinaga K. ¹⁸F-Fluoro-2-deoxyglucose positron emission tomography in cardiac sarcoidosis. *Eur J Nucl Med Mol Imaging*. 2011;38:1773–1783.